From Mott state to superconductivity in-1T-TaS

From Mott state to superconductivity in 1T-TaS$_2$

B. Sipos[*1], A.F. Kusmartseva[*1], A. Akrap[1], H. Berger[1], L. Forró[1], E. Tutiš[2]

[1] Faculté des Sciences de Base, EPFL, CH-1015 Lausanne , Switzerland

[2] Institute of Physics, Bijenička c. 46, Zagreb, Croatia

September 18, 2008

The search for the coexistence between superconductivity and other collective electronic states in many instances promoted the discovery of novel states of matter. The manner in which the different types of electronic order combine remains an ongoing puzzle. 1T-TaS$_2$ is a layered material, and the only transition metal dichalcogenide (TMD) known to develop the Mott phase. Here, we show the appearance of a series of low temperature electronic states in 1T-TaS$_2$ with pressure: the Mott phase melts into a textured charge density wave (CDW); superconductivity develops within the CDW state, and survives to very high pressures, insensitive to subsequent disappearance of the CDW state and, surprisingly, also the strong changes in the normal state. This is also the first reported case of superconductivity in pristine 1T-TMD compound. We demonstrate that superconductivity first develops within the state marked by a commensurability driven, Coulombically frustrated, electronic phase separation.

There is a long-standing enigma addressing the competition, coexistence or cooperation between various electronic collective states, in particular centring on the superconducting state. The most interesting systems from this point of view are those of reduced electronic dimensionality, that are more prone to electronic instabilities. Prominent examples include superconductivity in high temperature copper-oxide superconductors,[1–3] organic charge transfer salts,[4] heavy fermion compounds,[5] superconducting cobaltate systems[6] and some transition metal dichalcogenides.[4,7,8]

1T-TaS$_2$ is a rare layered material where both the Mott state and a number of peculiar charge density wave phases have been documented,[9–12] indicating that the electron-phonon and the electron-electron interactions are equally important in the shaping of its physics. Recent ARPES experiments have suggested a further anti-ferromagnetic ordering at low temperatures.[13]

The addition of superconductivity to this assortment of phases makes this material an important candidate for providing further insights into possible relations between electronic collective states in solids. The pressure-temperature phase diagram developed here for 1T-TaS$_2$ is unique in several respects. Combining our findings with the results of previous studies at ambient pressure, we report and explain the surprising observation of a superconducting state, that remains insensitive to the dramatic changes developing in the normal state under pressure.
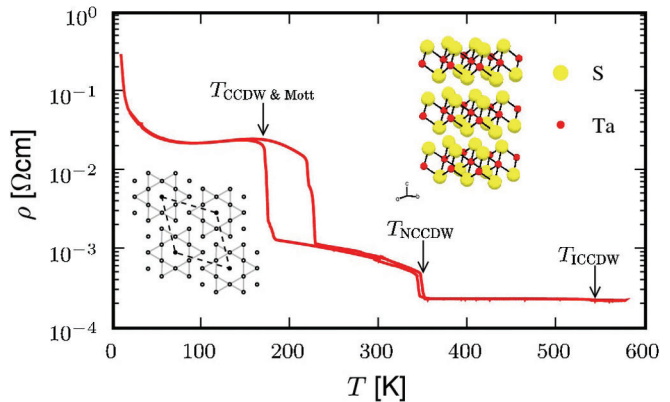
Figure 1: **Ambient pressure phases of 1T-TaS$_2$.** The phases are: a metallic phase at temperatures above 550 K; a charge density wave phase (ICCDW) above 350 K; a nearly commensurate charge density wave phase (NCCDW) above 190 K; a commensurate charge density wave CCDW Mott phase below 190 K; additionally there is a trigonal phase present solely during the warming up cycle between 200–300 K.[9,10,19] Also shown are the Ta atom distortions in the fully commensurate phase (see insert at low temperatures) and the crystal structure of 1T-TaS$_2$.

On the quantitative side, we show that the textured phase where the superconductivity first occurs is a state of commensurability-driven and Coulombically-controlled electronic phase separation. In this microscopic phase mixture, one phase supports the superconductivity, while the presence of the second phase severely affects the normal state properties.

The pressure is used here as an ideal tool to influence the electronic interactions within the material without

1

increasing the degree of internal disorder. This provides an obvious advantage over the usual and often complementary method of affecting the electronic system by chemical doping. The past studies prove that the pressure is especially successful in inducing changes in the electronic ground states for systems with reduced dimensionality,.[14–18] The case of 1T-TaS$_2$ adds to this list, with its unique features.

1   The starting point

1T-TaS$_2$ has a simple crystal structure, composed of planes of tantalum (Ta) atoms, surrounded in an octahedral arrangement by sulphur (S) atoms, see insert on Fig. 1. Even at ambient pressure, a variety of phases are present including a metallic phase at high temperatures, an incommensurate charge density wave (ICDW) phase below 550 K, a nearly commensurate charge density wave (NCCDW) phase below 350 K, and a commensurate charge density wave (CCDW) phase below 180 K. The charge density wave (CDW) state in 1T-TaS$_2$ is mostly driven by the Fermi surface instability, resembling the ones found in Peierls (quasi) one dimensional systems. The Peierls-like behaviour in 1T-TaS$_2$ is, however, substantially more complex.

The CCDW phase is geometrically the simplest among the CDW phases in this material. The displacement of the atoms leads to the formation of David star clusters, where twelve Ta atoms within the layer move inwards toward a thirteenth central Ta atom. The stars interlock by forming a triangular superlattice (Fig. 1, insert). However, this deformation does not fully gap the electronic system, with only twelve out of the thirteen electrons of the new unit cell occupying the electronic states below the energy gap created by the deformation. The "thirteenth" electron presides above the deformation-induced gap.[20] The enigma of high resistivity of this phase was resolved by pointing out that the system stabilizes by simultaneously developing a Mott insulator state from the electrons above the gap,[11,12] latter confirmed by other experiments including spectroscopic methods.[21,22] It should be noted that the formation of the David-star clusters also involves displacements perpendicular to the plane, causing a periodic swelling of the TaS$_2$ layers.[23,24] This CCDW-Mott phase was found to be sensitive to doping,[21,25] disorder induced by irradiation,[26] and pressurization.[27]

The neighbouring NCCDW phase equally contains David star clusters, although they are arranged in a less uniform manner.[9] Ambient pressure X-ray studies in 1T-TaS$_2$ reveal that in the NCCDW phase several tens of stars organize into roughly hexagonal domains, locally reproducing the CCDW phase.[10,28] The domains are separated by triangular regions where the amplitude of the deformation is reduced, forming the planar structure that resembles the Kagome patchwork.[10,28]

(a)

(b)
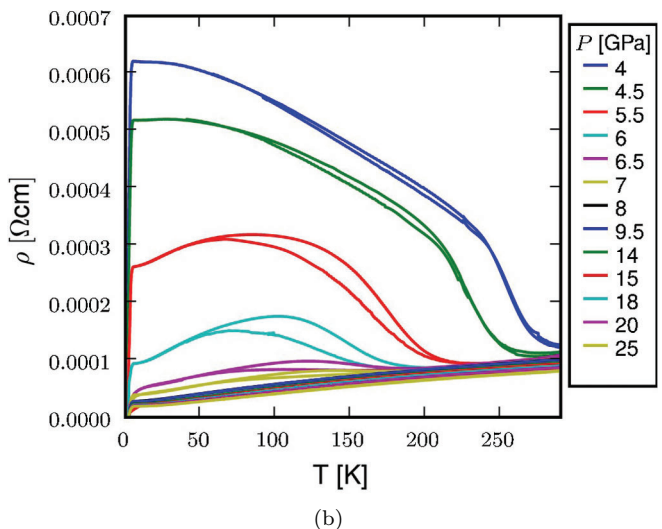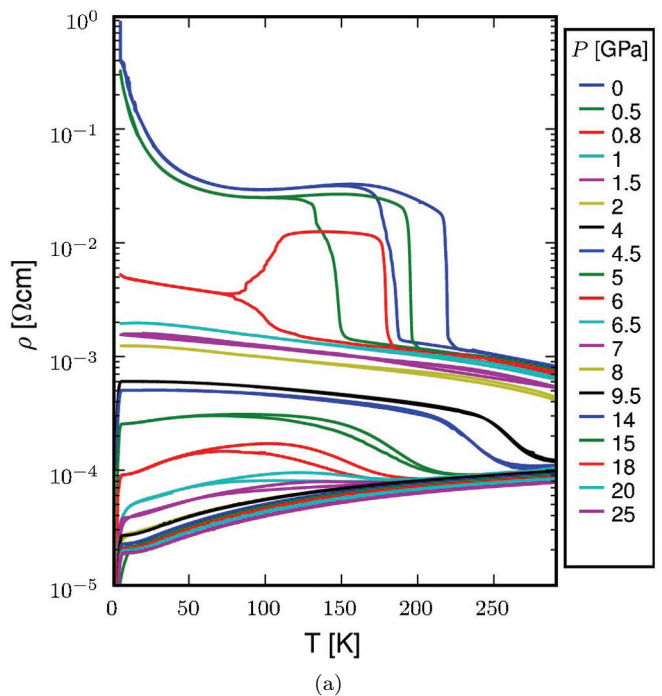
Figure 2: **Resistivity in the pressure range of 0–25 GPa and temperature range of 1.3–300 K.** Figure **a** shows that the temperature dependence of the resistivity is largely non-metallic over the entire temperature range for pressures of 0–4 GPa; the low temperature upturn in the resistivity that relates to the variable-range-hopping conduction in the Mott phase[11,12] disappears above 0.6 GPa; first traces of the superconductivity are observed at an approximate pressure of 2.5 GPa, with a T_{SC} of 1.5 K; metallic-like behaviour develops for low temperatures at pressures of 4–8 GPa; fully metallic behaviour is present at pressures greater then 8 GPa. Figure **b** clearly demonstrates that the superconductivity first develops with pressure within the non-metallic phase.

2 Experimental results

We have carried out resistivity measurements on 1T-TaS$_2$ under pressures ranging from 0–25 GPa and temperatures ranging from 1.3–300 K (Fig. 2(a)).

At temperatures below 250 K we observe a first order transition from the NCCDW to the CCDW phase at temperatures below 250 K, which melts with a pressure of 0.8 GPa. At low temperatures the resistivity saturates to finite residual values that shift lower and lower as the pressure is increased. The transition from the incommensurate to the nearly commensurate CDW phase appears as an increase in the resistivity in the temperature range of 120–300 K for the whole pressure range. The first confirmed signatures of superconductivity appear at 1.5 K and 2.5 GPa. The superconductivity arises from the *non-metallic* low temperature phase, which continuously evolves from the NCCDW state at ambient pressure.

In addition, at around 4-5 GPa, the resistivity saturates to a plateau-like temperature dependence below 50 K. The value of this low temperature residual resistivity drops as the pressure increased, and a metallic-like signature stabilises in the low temperature ranges. Above 8 GPa, the resistivity is metallic over the entire investigated temperature range, although the temperature dependence remains unconventional.

We summarize our findings in a pressure-temperature phase diagram (Fig. 3). The Mott localization and the CCDW phase are fully suppressed at pressures of about 0.8 GPa. The NCCDW phase persists to pressures of 7 GPa and may be visualised as roughly hexagonal CDW domains suspended in an interdomain phase.[10,28] The domains are expected to become progressively smaller as the pressure increases. The first signatures of superconductivity appear in the NCCDW phase and remain roughly at 5 K throughout the entire pressure range of 3–25 GPa. For pressures of 8–25 GPa the system is metallic over the investigated temperature range when above the superconducting transition temperature. Recent preliminary field measurements indicate that the critical magnetic field would be of the order of 1.5 T, in the lower pressure ranges.

The questions which emerge from this new phase diagram address the melting of the CCDW Mott state, the origin of the textured NCCDW phase in relation to that state, the appearance of superconductivity in a pristine 1T system, which remains apparently insensitive to both pressure and the melting of the charge order.

3 Discussion

The exceptional assembly of electron-phonon coupling, nesting effects and Coulomb interaction combine to construct the elaborate phase space of 1T-TaS$_2$. In order to understand the many complexities of this system it is important to consider the microscopics of the different phases at ambient pressure and their possible evolution under pressure. We will address each of the above posed questions separately.

3.1 Meltdown of the Mott phase

The standard way of influencing the Mott phase is to affect the ratio between the Coulomb repulsion and the bandwidth. These two relevant energy scales correspond to the parameters U and t of the single-band Hubbard Hamiltonian, usually used to consider the Mott transition,

$$H = -t \sum_{\langle i,j \rangle, \sigma} \left(c_{i,\sigma}^\dagger c_{j,\sigma} + c_{j,\sigma}^\dagger c_{i,\sigma} \right) + U \sum_i n_{i,\uparrow} n_{i,\downarrow}$$

where $c_{i,\sigma}$ and $c_{i,\sigma}^\dagger$ are the destruction and creation operators of an electron at site i and with spin σ, and $n_{i,\sigma} = c_{i,\sigma}^\dagger c_{i,\sigma}$ is the occupation operator. For the special case of the triangular lattice of David stars in 1T-TaS$_2$, t and U map to the overlap of the electronic wave functions defined by the deformation localized at David stars, and the Coulomb interaction of the electrons above the gap within the same David star, respectively.

The qualitative understanding of the observed phase transition comes from the insight that pressure changes both the relevant energy scales, by decreasing the swelling of the planes related to the David star deformations in the CDW state. In particular, by reducing the deformation, the pressure diminishes the CDW gap and increases the screening capacity of the electrons below the gap (i.e. the inter-band contribution to the dielectric function)). Similarly, the pressure also weakens the potential that defines the local wavefunction, thereby increasing its extension and the wavefunction overlap integral. Both these mechanisms simultaneously increase t and decrease U, leading to a decrease in the ratio U/t. The Mott state melting occurs naturally at a critical value of this ratio.[29]

3.2 Nature of the textured phase

The NCCDW phase has been subject to numerous experimental and theoretical investigations at ambient pressure. Previous theoretical approaches invoked mainly phenomenological treatments, based on sophisticated versions of the Landau-type functional, leaving out the microscopic details.[30,31] However, the main mechanism behind the creation of the textured phase has been established to lie in the tendency of the system to maximize the electronic gap at a given deformation amplitude by (inter)locking the deformations at (three) commensurate wave-vectors, counteracted by the remnant part of the electrons in the states above
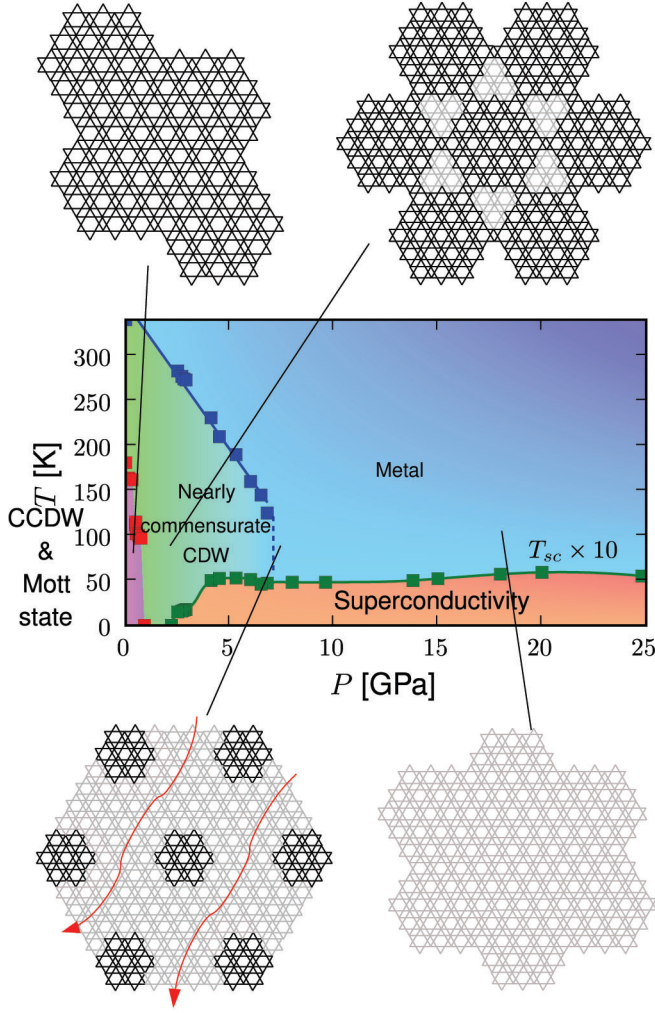
Figure 3: **The temperature-pressure phase diagram of 1T-TaS$_2$.** The Mott localization is suppressed, closely accompanied by the melting of the commensurate CDW phase at a pressure of 0.8 GPa; the lattice structure in the latter phase is composed of interlocking David stars. The nearly commensurate CDW phase extends over the pressure range of 1–7 GPa, and may be visualised as roughly hexagonal domains suspended in an interdomain phase, indicated in grey. The first signatures of superconductivity appear from the nearly commensurate CDW state, and remain roughly at 5 K throughout the entire pressure range of 3–25 GPa. In the pressure range of 8–25 GPa the system is metallic over the investigated temperature range when above the superconducting transition temperature. The drawing above and below the phase diagram indicates the probable deformation patterns in the system at low temperature, as discussed in the text. Darkly shaded parts denote the parts with the static deformation in the form of David stars, while in the light-shaded areas the deformation is considerably reduced or completely suppressed.

the gap. This leads to a microscopic mechanism for domain formation, common to many electronic systems with (charge or spin) density waves close to commensurability.[32] Essentially, the discommensurations in the textured phase host the electrons that do not fit below the gap that exists in the commensurately ordered domains. Notably, however, the size of the domains in 1T-TaS$_2$ is substantial, containing several hundred of TaS$_2$ units within each layer. Therefore, long range Coulomb forces are expected to control the charge transfer involved in the domain size and organization.[33] This important aspect was omitted in former theoretical treatments of the NCCDW phase in 1T-TaS$_2$.

We fully include the Coulomb aspect of this charge transfer, when considering the formation of domains in the NCCDW phase in 1T-TaS$_2$. The two limiting degrees of this charge relocation leave the domains either as a lightly (self-)doped Mott state, or fully depleted. We compare the Coulomb energy per particle involved in the formation of fully depleted domains, E_c with the electronic energy gap Δ in the domains. The case of $E_c \sim \Delta$ implies a Coulomb controlled textured phase. The alternatives, unrestricted by the long range Coulomb forces, relate to $E_c \ll \Delta$ and $E_c \gg \Delta$ signifying fully depleted and slightly doped Mott phase domains, respectively. Fig. 4 shows the results of a calculation, for different domain sizes and organization in successive layers. The calculation (see Methods) is performed for a Kagome patchwork with two different stacking alignments. Stacking A considers an axial alignment of domains and interdomain triangles in successive layers, and has been experimentally observed in 1T-TaS$_2$ (see Fig. 4, Stacking A). The shifted positions of the domains between adjacent planes resemble a closely packed face centred cubic (FCC) structure.[28] Stacking B refers to a hypothetical case of an exact axial superposition of the domains between the planes, for comparison (see Fig. 4, Stacking B). We show that the deviation from the observed Stacking A structure induces a big change in the Coulomb energy. The calculations demonstrate that the experimentally observed stacking and sizes of the domains support Coulomb controlled texturing and depletion of the domains.

We conclude that the NCCDW phase of 1T-TaS$_2$ at ambient pressure, is an example of a Coulombically controlled and commensurability driven electronic phase separation. This state extends to very low temperature upon pressurization, where superconductivity occurs.

3.3 Superconductivity in the textured phase

Within the conventional picture, the CDW and superconducting ground states compete against each other, because both result in a gapping of the single-particle electronic spectra at the Fermi level. Indeed, the super-

conductivity in 1T-TaS$_2$ appears as soon as the fully commensurate CDW phase is suppressed at low pressures of 0.8-1 GPa, suggesting a mutual exclusion of each other. On the other hand, no notable competition is observed in the pressure range of 1–7 GPa within the NCCDW phase where the CDW and superconductivity coexist.

To illustrate this point we consider the behaviour of the normal-state resistivity as a function of pressure (Fig. 5). Technically, we take the normal-state or the residual resistivity to be the resistivity at 6 K above 1 GPa. Below that pressure the resistivity is dominated by a variable range-hopping regime in the Mott state, (see Fig. 2(a)). The residual resistivity decreases gradually above 1 GPa until an approximate pressure of 4 GPa. This may be explained by the shrinking of the CDW domains with pressure and an increased fraction of electrons in the interdomain phase. In the pressure range of 4–7 GPa, we see a shoulder-like anomaly in this effective residual resistivity. This probably indicates a complete dissociation of the CDW domains into a uniform, fluctuating background of weak distortions. Above 7 GPa the pressure dependence of the residual resistivity is less significant.
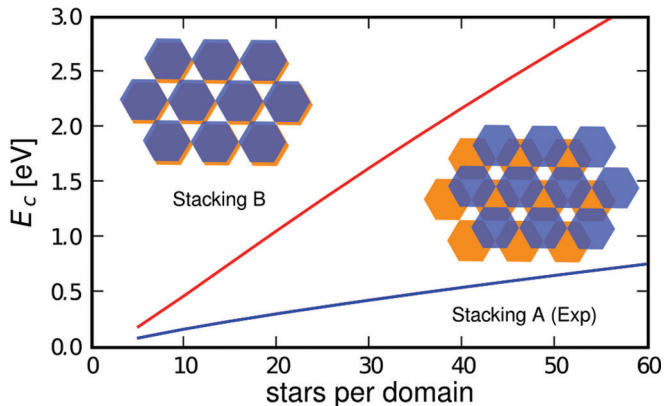

Figure 4: **The results for the Coulomb energy calculation for two different domain stacking as a function of domain size**. The lower line (blue), corresponds to an axial arrangement of domains (hexagonal) and interdomain spaces (triangular) between adjacent layers (stacking A), as deduced from experiment;[28] the upper line (red) shows, for comparison, the Coulomb energy for a hypothetical axial domain stacking between successive layers (stacking B). The green dashed box depicts the values of domain sizes that were experimentally observed in the NCCDW phase at ambient pressure. We note that the Coulomb energies calculated for these values are comparable to the energy of the gap, hinting at a possible Coulomb-controlled phase separation.

Naturally, we propose the assumption that the su-

perconductivity forms within the metallic interdomain spaces of the NCCDW phase. Thereby, remarkably, the competition between the CDW and superconductivity is avoided in the NCCDW phase through a phase separation in real space on a microscopic scale. Thus, the superconducting state remains rather insensitive to the size, and even the disappearance of the domains brought on by the pressure change. On the contrary, we may assume that the domains appear as scatterers of the electrons in the normal state, which would explain the manifest sensitivity of the normal-state resistivity to the collapse of the CCDW domains around a pressure of 7 GPa (Fig. 5).

We may postulate that the electron-phonon coupling that is inherent in the CDW state vastly helps the superconductivity in undeformed parts of the system. Combined with the phase separation on microscopic level, this would lead to the conclusion that the same parts of the Fermi surface are being affected by the CDW and the superconductivity transitions. This has been recently observed in 2H-NbSe$_2$[34] — another member of the TMD compounds, where an analogous indifference of the superconductivity with respect to the CDW transition has been detected,[4] with some evidence for a textured phase based on a triple CDW state.[35, 36]

It may be informative to consider the effect of intercallation on the charge density wave in this material. Intercalation increases the spacing between layers, which may be beneficial for the deformation related to the Mott state phase and at the same time introduces spurious charge carriers which are likely to suppress this Mott state phase. Whether the intercalation would give rise to the currently observed superconducting phase is unclear.

3.4 Compete or coexist?

There are several pictures relating charge ordering and superconductivity that exist in the literature. These prove inconsistent with our phase diagram. We rule out the possibility of superconductivity rooted in a manner of a self-doped Mott phase.[2, 37] This scenario is unlikely because of a significant charge transfer from the CCDW domains to the interdomain space within the NCCDW phase, and the insensitivity of the superconductivity to the disappearance of the CDW state. For that same reason, no signs of charge or spin-ordering fluctuations facilitating superconductivity are established to be present in 1T-TaS$_2$ contrary to some other low-dimensional materials.[38, 39] On the other hand, our phase diagram of 1T-TaS$_2$ is remarkably similarly to that of some of the organic layered superconductors κ-(BEDT-TTF)$_2$X,[18] although on a different pressure scale. Recent studies have uncovered numerous similarities, especially those revolving around the appearance
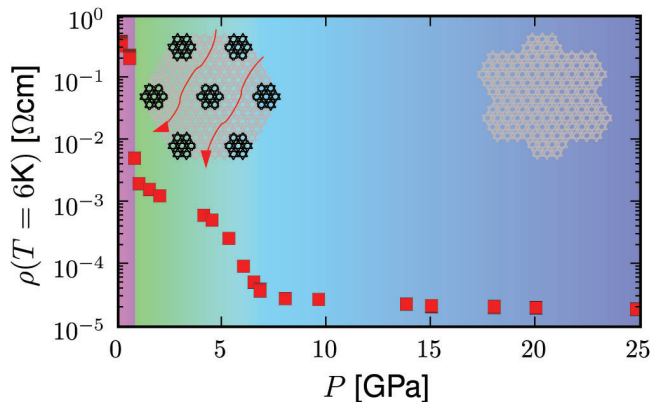
Figure 5: **Resistivity taken at a temperature of 6 K as a function of pressure**. Sharp decrease in resistivity accompanies the suppression of the Mott-localised phase; linear residual resistivity pressure dependence accompanies the gradual melting of the CDW domains in the nearly commensurate CDW phases; a shoulder-like anomaly in the pressure range 4–7 GPa may be associated with the complete dissociation of the CDW domains with pressure; above 7 GPa the residual resistivity again behaves linearly with pressure. The scattering of electrons on the CCDW islands dominate the resistivity below 7 GPa

of the pseudogap, between the layered organics, the superconducting cuprates and several dichalcogenide superconductors, advocating separate origins for the pseudogap and the superconducting gap.[40,41] 1T-TaS$_2$ may be sited within this framework by the presence of two types of order presumably accompanied by two distinct gaps in the pressure region between 1 GPa and 7 GPa. In addition, the relation between the electronic phase separation and superconductivity has been extensively considered for the cuprate systems in the form of stripes,[3,42,42–44] and recently observed by scanning tunneling microscopy.[45]

In conclusion, the coincidental occurrence of both the Mott state, commensurate charge density wave phase (CCDW) and superconductivity in 1T-TaS$_2$ presents unequivocal opportunities to investigate these collective states of matter in relation to each other. The balance between these several regimes, spanning from the localized CCDW Mott phase to unconventional metallic states is readily and controllably tuneable by the application of external pressure. Although the superconductivity in 1T-TaS$_2$ shares a few common features with the superconductivity in a number of layered superconductors that have been subject to extensive interest in recent years, there are a number of key differences. The remarkable insensitivity of the superconducting phase to the changes in the normal states; the development of a Mott phase at low pressures as well as an exceptional

variety of CDW phases, among those the textured non-metallic phase that hosts superconductivity, all combined stress the underlying importance of this material in the still perplexing field of electronic collective phenomena. In the future the 1T-TaS$_2$ would particularly benefit from further clarification of the normal and the superconducting states under pressure, utilising X-ray structural studies, Raman and infrared studies.

4 Methods

4.1 Measurements

The resistivity was measured using a standard 4-point technique, with an AC current of 5 mA and a frequency 16.98 Hz. Pressure measurements in the low pressure range 0–2 GPa were obtained in a standard piston cylinder pressure cell. Pressure measurements in the pressure range 2–25 GPa were performed in an opposed anvil Bridgeman-type pressure cell with tungsten carbide, sintered diamond anvils and quasi-liquid steatite medium. Pressure was determined, using a standard lead pressure gauge. A pumped helium cryostat was used to achieve base temperatures of 1.3 K.

4.2 Calculating Coulomb energy

The Coulomb energy related to the charge transfer within the superstructure shown in Fig. 4 is calculated starting from the usual expression,

$$E_{\text{Coul}} = \frac{1}{2} \int_{\text{s.c.}} d^3\overrightarrow{r} \int d^3\overrightarrow{r'} \frac{1}{4\pi\varepsilon_0\varepsilon_r} \frac{\rho(\overrightarrow{r})\rho(\overrightarrow{r'})}{\left|\overrightarrow{r} - \overrightarrow{r'}\right|},$$

where the first integral goes over the supercell in the TaS$_2$ plane, while the second integral goes over the whole space. $\rho(r)$ stands for the charge density produced by the charge transfer from domains to inter-domain space. E_{Coul} stands for the energy per supercell in the TaS$_2$ plane, while the energy E_c per electron transferred is obtained by dividing E_{Coul} by the number of David stars in the domain. Given the particular shape of the textured phase, we choose to calculate the integral in direct space, though with some simplifications. Firstly, being only interested in the long-wavelength aspect of the charge transfer, we do not consider the details of the charge distribution vertically within the layer, or on the scale of the basic TaS$_2$ cell. Accordingly, the Coulomb potential is regularized below distance d, of the order of the separation between two neighbouring Ta atoms, and the planar charge density is assumed smooth on that scale. The latter is set within the domain by the requirement of one electron lacking per David star, and the requirement that each supercell remains neutral. Additionally, no variation in planar charge density is allowed within domains

or within the inter-domain space. The former integral then transforms into the three-dimensional sum of convolutions of planar integrals over pairs of planar supercells. The sum is rapidly converging upon choosing the high-symmetry supercell, while all integrals are numerically calculated by subdividing the planar supercell into small triangles (size of the order of d). The requirement that the states above the gap in domains are kept void, determines the contributions to the dielectric constant ε_r that enters the calculation. Specifically, the contribution from electrons from metallic, "triangular" parts should be excluded, and only the contributions that relate to gapped charge-density wave should be included. Since these contributions also determine the screening of the electron-electron interaction in the Mott phase, the approximate value for appropriate ε_r may be determined from the proximity of that phase. The collapse of the Mott state on triangular lattice[29] is known to occur at $U/t \sim 10$. The value of U is given by $e^2/r_{DS}\varepsilon_r$, where r_{DS} is of the order of the radius of the David star in 1T-TaS$_2$, $e^2/r_{DS} \sim 2$ eV. The transfer integral t relevant for the Hubbard model one may read from the relevant band-width W in the band structure calculation,[20] $W = 8t \approx 0.1$ eV. This leads to $\varepsilon_r \sim 10$, used in our calculation.

References

[1] Bednorz, J. G. & Müller, K. A. Possible high T_c superconductivity in the Ba-La-Cu-O system. *Zeitschrift für Physik B Condensed Matter* **64**, 189–193 (1986).

[2] Lee, P. A., Nagaosa, N. & Wen, X.-G. Doping a Mott insulator: Physics of high-temperature superconductivity. *Rev. Mod. Phys.* **78**, 17–76 (2006).

[3] Carlson, E., Emery, V., Kiveslon, S. & Ograd, D. *The Physics Of Conventional And Unconventional Superconductors* (Springer-Verlag, Berlin, 2003).

[4] Gabovich, A. M., Voitenko, A. I., Annett, J. F. & Ausloos, M. Charge- and spin-density wave superconductors. *Sup. Sci. and Tech.* **14**, R1–R27 (2001).

[5] Grosche, F. M. et al. Superconductivity on the threshold of magnetism in cepd2si2 and cein3. *Journal of Physics: Condensed Matter* **13**, 2845–2860 (2001).

[6] Takada, K. et al. Superconductivity in two-dimensional CoO$_2$ layers. *Nature* **422**, 53–55 (2003).

[7] Morosan, E. et al. Superconductivity in Cu$_x$TiSe$_2$. *Nat. Phys.* **2**, 544–550 (2006).

[8] Friend, R. H. & Yoffe, A. D. Electronic properties of intercalation complexes of the transition metal dichalcogenides. *Adv. in Phys.* **36**, 1–94 (1987).

[9] Wilson, J. A., Di Salvo, F. J. & Mahajan, S. Charge density waves and superlattices in metallic layered transition-metal dichalcogenides. *Adv. in Phys.* **24**, 117–201 (1975).

[10] Thomson, R. E., Burk, B., Zettl, A. & Clarke, J. Scanning tunneling microscopy of the charge-density-wave structure in 1T-TaS$_2$. *Phys. Rev. B* **49**, 16899–16916 (1994).

[11] Fazekas, P. & Tosatti, E. Charge carrier localization in pure and doped 1T-TaS$_2$. *Physica B & C* **99**, 183–187 (1980).

[12] Fazekas, P. & Tosatti, E. Electrical, structural and magnetic-properties of pure and doped 1T-TaS$_2$. *Philos. Mag. B* **39**, 229–244 (1979).

[13] Perfetti, L., Gloor, T. A., Mila, F., Berger, H. & Grioni, M. Unexpected periodicity in the quasi-two-dimensional Mott insulator 1T-TaS$_2$ revealed by angle-resolved photoemission. *Phys. Rev. B* **71**, 153101 (2005).

[14] Bourbonnais, C. & Jrome, D. *Advances In Synthetic Metals* (Elsevier, New York, 1999).

[15] Ramirez, A. C$_{60}$ and its superconductivity. *Supercond. Rev* **1**, 1–101 (1994).

[16] Zhou, O. et al. Structural and electronic properties of (NH$_3$)×K$_3$C$_6$0. *Phys. Rev. B* **52**, 483–489 (1995).

[17] Ishiguro, T., Yamaji, K. & SaitoT, G. *Organic Superconductors* (Springer-Verlag, Berlin, 1998).

[18] Nam, M.-S., Ardavan, A., Blundell, S. J. & Schlueter, J. A. Fluctuating superconductivity in organic molecular metals close to the Mott transition.

Nature **449**, 584–587 (2007).

[19] Isa, T. et al. Charge density wave domain originated Altshuler-Aronov-Spivak effect in 1T-TaS$_2$ single crystal. *Physica Status Solidi (b)* **229**, 1111 (2002).

[20] Rossnagel, K. & Smith, N. V. Spin-orbit coupling in the band structure of reconstructed 1T-TaS$_2$. *Phys. Rev. B* **73**, 073106 (2006).

[21] Zwick, F. et al. Spectral consequences of broken phase coherence in 1T-TaS$_2$. *Phys. Rev. Lett.* **81**, 1058–1061 (1998).

[22] Pillo, T. et al. Interplay between electron-electron interaction and electron-phonon coupling near the Fermi surface of 1T-TaS$_2$. *Phys. Rev. B* **62**, 4277–4287 (2000).

[23] Wilson, J. A. Questions concerning the form taken by the charge density wave and the accompanying periodic-structural distortions in 2H-TaSe$_2$, and closely related materials. *Phys. Rev. B* **17**, 3880–3898 (1978).

[24] Bovet, M. et al. Interplane coupling in the quasi-two-dimensional 1T-TaS$_2$. *Phys. Rev. B* **67**, 125105 (2003).

[25] Di Salvo, F. J., Wilson, J. A., Bagley, B. G. & Waszczak, J. V. Effects of doping on charge density waves in layer compounds. *Phys. Rev. B* **12**, 2220–2235 (1975).

[26] Mutka, H., Zuppiroli, L., Molinié, P. & Bourgoin, J. C. Charge-density waves and localization in electron-irradiated 1T-TaS$_2$. *Phys. Rev. B* **23**, 5030–5037 (1981).

[27] Tani, T., Osada, T. & Tanaka, S. The pressure effect on the CDW-transition temperatures in 1T-TaS$_2$. *Solid State Commun.* **22**, 269–272 (1977).

[28] Spijkerman, A., de Boer, J. L., Meetsma, A., Wiegers, G. A. & van Smaalen, S. X-ray crystal-structure refinement of the nearly commensurate phase of 1T-TaS$_2$ in $(3 + 2)$-dimensional super-space. *Phys. Rev. B* **56**, 13757–13767 (1997).

[29] Capone, M., Capriotti, L., Becca, F. & Caprara, S. Mott metal-insulator transition in the half-filled Hubbard model on the triangular lattice. *Phys. Rev. B* **63**, 085104 (2001).

[30] McMillan, W. L. Theory of discommensurations and the commensurate-incommensurate charge density wave phase transition. *Phys. Rev. B* **14**, 1496–1502 (1976).

[31] Nakanishi, K. & Shiba, H. Theory of 3-dimensional orderings of charge density waves in 1T-TaS$_2$. *J. Phys. Soc. Jpn.* **53**, 1103-1113 (1984).

[32] Brazovskii, S. Solitons and their arrays: From quasi 1D conductors to stripes. *Jour. Of Sup. Cond. And Nov. Mag.* **20**, 489–493 (2007).

[33] Miranda, J. & Kabanov, V. Coulomb frustrated first order phase transition and stripes. *Physica C* **468**, 358–361 (2008).

[34] Kiss, T. et al. Charge-order-maximized momentum-dependent superconductivity. *Nat. Phys.* **3**, 720–725 (2007).

[35] Moncton, D. E., Axe, J. D. & Di Salvo, F. J. Study of superlattice formation in 2H-NbSe$_2$ and 2H-TaSe$_2$ by neutron scattering. *Phys. Rev. Lett.* **34**, 734–737 (1975).

[36] Sacks, W., Roditchev, D. & Klein, J. Voltage-dependent STM image of a charge density wave. *Phys. Rev. B* **57**, 13118–13131 (1998).

[37] Baskaran, G. Mott insulator to high T_c super-conductor via pressure: resonating valence bond theory and prediction of new systems. *Phys. Rev. Lett.* **90**, 197007 (2003).

[38] Merino, J. & McKenzie, R. H. Superconductivity mediated by charge fluctuations in layered molecular crystals. *Phys. Rev. Lett.* **87**, 237002 (2001).

[39] Jérome, D. The physics of organic superconductors. *Science* **252**, 1509–1514 (1991).

[40] Klemm, R. A. Striking similarities between the pseudogap phenomena in cuprates and in layered organic and dichalcogenide superconductors. *Physica C* **341-348**, 839–842 (2000).

[41] McKenzie, R. H. Similarities between organic and cuprate superconductors. *Science* **278**, 820–821 (1997).

[42] Emery, V. J. & Kivelson, S. A. Frustrated electronic phase separation and high-temperature superconductors. *Physica C: Superconductivity* **209**, 597–621 (1993).

[43] Müller, K. A. & Benedek, G. (editors). *Phase Separation In Cuprate Superconductors* (World Scientific, Singapore, 1993).

[44] Kivelson, S. A. et al. How to detect fluctuating stripes in the high-temperature superconductors. *Rev. Mod. Phys.* **75**, 1201–1241 (2003).

[45] Kohsaka, Y. et al. An intrinsic bond-centered electronic glass with unidirectional domains in underdoped cuprates. *Science* **315**, 1380–1385 (2007).

5   Acknowledgements

6   Author contribution

A. F. K. and B. S. shared equal responsibility for all aspects of this project from sample preparation to data collection and analysis. A. A. did part of the low pressure measurements. H. B. grew the samples. E. T. contributed to the theoretical aspects of the discussions and performed the calculations. L. F. was the overall project leader who initiated the topic and advised the research.